

Mid-Fidelity Framework for Rotor Noise Prediction and Perception in Maneuvering flight

Original

Mid-Fidelity Framework for Rotor Noise Prediction and Perception in Maneuvering flight / Picillo, Marco; Barbarino, Mattia; Avallone, Francesco. - (2025), pp. 1447-1455. (Forum Acusticum Euronoise 2025. 11th Convention of the European Acoustics Association Malaga (ESP) 23-26 June 2025) [10.61782/fa.2025.0567].

Availability:

This version is available at: 11583/3001534 since: 2025-07-04T07:14:15Z

Publisher:

EAA

Published

DOI:10.61782/fa.2025.0567

Terms of use:

This article is made available under terms and conditions as specified in the corresponding bibliographic description in the repository

Publisher copyright

(Article begins on next page)



FORUM ACUSTICUM EURONOISE 2025

MID-FIDELITY FRAMEWORK FOR ROTOR NOISE PREDICTION AND PERCEPTION IN MANEUVERING FLIGHT

Marco Picillo^{1*}

Mattia Barbarino²

Francesco Avallone¹

¹ Department of Mechanical and Aerospace Engineering, Politecnico di Torino, Italy

² Centro Italiano Ricerche Aerospaziali, Capua, Italy

ABSTRACT

The goal of Urban Air Mobility (UAM) is to provide a safe, efficient, and sustainable transportation option to reduce traffic congestion and improve mobility in cities. However, the benefits, such as reduction of pollution and increase of public health, need to face important challenges related to safety, regulatory frameworks and public acceptance; the latter is highly driven by noise emissions. In this paper a mid/low-fidelity framework is used to investigate the effects of the acceleration between two steady conditions at different angular velocities for a small propeller. Far-field noise results are evaluated in terms of physical and psychoacoustic metrics. Differences in amplitude and directivity patterns suggest that in the presence of a fast transient, noise increases. Different angular velocity accelerations have also been investigated, highlighting their impact on noise perception.

Keywords: *Noise, UAM, Maneuver, Perception*

1. INTRODUCTION

Urban Air Mobility (UAM) refers to the use of advanced air transportation systems, including electric Vertical Takeoff and Landing (eVTOL) aircraft, to transport people and goods within urban and suburban areas. Beside this concept, Advanced Air Mobility (AAM) encompasses a range of new and emerging technologies in avi-

ation, including UAM, but also includes larger and faster aircraft that are capable of longer-range flights. The development of these new concepts has been accelerated, in the recent years, thanks to the technological advance of VTOL, which are vehicles capable of take-off and landing in a small space [1] and are mainly driven by distributed propellers. Both AAM and UAM are expected to have significant impact on our future lives. However, the benefits, such as reduction of pollution, increase of public health and so on, need to face some important challenges related to safety, regulatory frameworks and public acceptance.

In the context of public acceptance, the analysis proposed by [2] shows that public acceptance is highly driven by noise. For this reason, it is crucial to correctly predict noise emissions from rotorcrafts in urban environments, which are characterized by non-uniform flows, gusts and turbulence [3], causing a non-uniform inflow condition at the rotor disk that determines a dramatic change in sound pressure levels and directivity [4]. Another important challenge is represented by the correct prediction of noise emissions in maneuvering flight and how noise is perceived by an observer. In order to predict noise emissions, different numerical methods are usually adopted, ranging from high-fidelity to low-fidelity. High-fidelity and low-fidelity approaches share the same philosophy, based on predicting blade loads and fluid displacement around the propeller, using an aerodynamic solver, which are then used to compute the acoustic pressure at a specific observer location. Classification is based on the accuracy of the aerodynamic and acoustic solvers that are used for the simulation. High-fidelity methods adopt high-fidelity Computational Fluid Dynamics (CFD) methods such as Reynolds Averaged Navier-Stokes (RANS) [5], Large Eddy Simulation (LES) [6] and Very Large Eddy

*Corresponding author: marco.picillo@polito.it.

Copyright: ©2025 Marco Picillo et al. This is an open-access article distributed under the terms of the Creative Commons Attribution 3.0 Unported License, which permits unrestricted use, distribution, and reproduction in any medium, provided the original author and source are credited.





FORUM ACUSTICUM EURONOISE 2025

Simulation (VLES) [4] to obtain near field description of noise sources, while the near to far field propagation is carried out by the Ffowcs Williams and Hawkins analogy (FW-H), which is a re-formulation of the linearized Euler equations using Lighthill's acoustic analogy [7]. On the other side, low-fidelity methods adopt low-fidelity CFD methods, such as Blade Element Momentum Theory (BEMT) [8], Lifting Line Theory (LLT) [9] and Potential Flow Methods [10] coupled with simplified versions of the FW-H equation such as Hanson's and Gutin's model in the frequency domain and Farassat 1 and 1A formulations in the time domain.

Although noise prediction for propellers in stationary and uniform-inflow conditions has been extensively studied, noise prediction from maneuvering rotorcraft remains a challenging problem. In practice, VTOLs and drones perform complex maneuvers. Rotorcraft flight, in general, can be described as a sequence of equilibrium states interspersed with transitional maneuvers. These maneuvers are marked by non-stationary and aperiodic effects, leading to noise generation mechanisms that significantly differs from the ones in stationary conditions [11]. This additional noise, which increases as the duration of the maneuver decreases, is not negligible as it is characterized by a time-dependent directivity [12].

The majority of studies in the literature employ a quasi-stationary approach, ignoring the transient that occurs when transitioning from one flight condition to another; only few works consider the effects of a short-time maneuver in terms of physical noise metrics. In [13] the noise of a helicopter transient maneuver is numerically simulated using the formulation 1A of Farassat, while [14] used a BEMT solver coupled with an acoustic solver, based on the formulation 1A of Farassat, to investigate the effects of a typical eVTOL mission on the noise of an observer fixed with the vehicle. However, most of the studies cited above focus primarily on physical noise metrics, such as Sound Pressure Level (SPL), while few address the effects of a short-time maneuver on noise perception. Ref. [15] highlights experimentally the effects of a drone transient flight in terms of sound quality metrics, such as loudness, sharpness and roughness with respect to the hovering case, while [16] focused on the effects of different type of propellers on the psychoacoustic annoyance, suggesting that perception-driven design can be performed by targeting the minimization of the perceived noise annoyance, rather than just reducing SPL. For this reason, with the aim of tackling the challenge of public acceptance, it is important to address the psychoacous-

tic effects of short-time maneuvers, in a fast and accurate way, due to the variety of eVTOL and drones architectures present in the market nowadays, and to include these metrics with the purpose of guiding future designs.

The purpose of this paper is to analyze the effects of angular velocity acceleration, for a small drone rotor, on physical and psychoacoustic metrics, using a low-fidelity framework. This paper is structured as follows: in Sec. 2 the simulation framework is introduced, in Sec. 3 a validation in uniform and non-uniform inflow conditions is presented, while in Sec. 4 the results of a short-time maneuver in terms of sound quality metrics and physical noise metrics will be discussed.

2. SIMULATION FRAMEWORK

In this section, the simulation framework is presented. The tool is composed of an aerodynamic solver, which is FLOWUnsteady [17], based on Vortex Particle Method and an in-house time-domain acoustic solver for the tonal component of the noise, based on the FW-H analogy [18]. The sketch, shown in figure Fig. 3, presents the workflow. First, the rotor geometry, defined with chord distribution, twist distribution, sweep distribution, rotor diameter, airfoils distribution and number of blades is passed to the aerodynamic solver, together with the operating conditions of the rotor. Then, the time history of the blade loading distribution along the radius of each blade is passed to the acoustic solver, together with the observer position, in order to compute a pressure signal at the observer position and finally the noise, in terms of physical noise metrics such as SPL and perception using the open-source python library MoSQUITO [19]. The acoustic solver is developed in Python, following the object-oriented paradigm, which make the software user-friendly and modular.

Vortex Methods are a class of meshless CFD solving the Navier-Stokes equations in their velocity-vorticity form. In particular, the method uses particles to discretize the Navier-Stokes equations. Each particle represents a Radial Basis Function that constructs a continuous vorticity field by carrying an integral quantity of vorticity that is convected by the velocity field. In FLOWUnsteady, blades are divided into blade elements that include 2D airfoil data, such as lift and drag, calculated by XFOIL. The forces on each blade are then reintroduced into the fluid domain by converting them into equivalent immersed vorticity. In this way, it is possible to compute the performance of one or multiple rotors under different operating conditions.





FORUM ACUSTICUM EURONOISE 2025

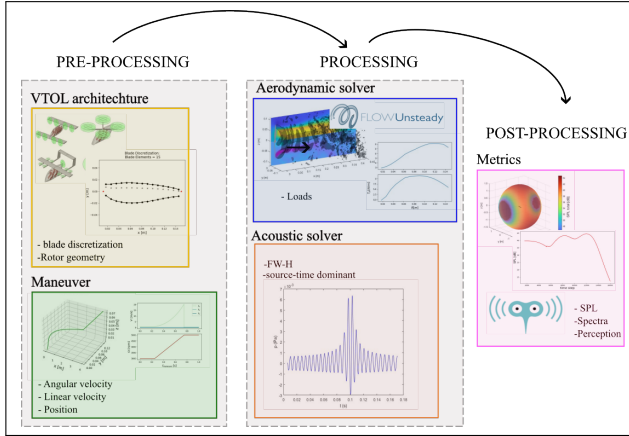


Figure 1. Simulation Framework.

For the acoustic solver we follow the procedure presented in [18]. Only the thickness and loading noise components are computed. More in detail, the FW-H equation, Eqn. (1), is simplified considering two hypotheses: observer placed in the far field and surface integrals calculated on the blade planform.

$$\begin{aligned} \rho'(\mathbf{x}, t)c_\infty^2 &= \frac{\partial^2}{\partial x_i \partial x_j} \int_{V_0} \left[\frac{\mathbf{T}_{ij}}{4\pi r |1 - M_r|} \right]_{\tau=\tau^*} dV(\mathbf{z}) \\ &- \frac{\partial}{\partial x_i} \int_{S_0} \left[\frac{p_{ij} \mathbf{n}_j}{4\pi r |1 - M_r|} \right]_{\tau=\tau^*} dS(\mathbf{z}) \\ &+ \frac{\partial}{\partial t} \int_{S_0} \left[\frac{\rho_\infty V_j \mathbf{n}_j}{4\pi r |1 - M_r|} \right]_{\tau=\tau^*} dS(\mathbf{z}) \end{aligned} \quad (1)$$

Each integrand is then evaluated at the retarded time τ^* which is the time needed to the signal, emitted at time τ , to reach the observer position at time t . The retarded time equation, Eqn. (2), is solved implicitly.

$$t - \tau - \frac{|\mathbf{x} - \mathbf{y}(\tau)|}{c_\infty} = 0 \quad (2)$$

where \mathbf{y} is the blade position in the fixed reference system, \mathbf{x} the observer position and c_∞ the speed of sound.

3. VALIDATION

In this section, the noise generated by a rotor in a uniform and non-uniform inflow is compared against high-fidelity and experimental data, in order to partially validate the numerical tool. The geometrical characteristics of the propeller and reference values used for the simulations are

summarized in Tab. 1, while geometric characteristics of the propeller can be seen in Fig. 2 and found in previous works from [20] and [4].

Table 1. Propeller parameters and reference values.

| | |
|-------------------------------|-----------------------|
| Propeller diameter (D) | 0.3 m |
| Hub to tip ratio | 0.13 |
| Number of blades (N_b) | 2 |
| Blade airfoils | NACA 4412 |
| Air density (ρ_∞) | 1.18 kg/m^3 |
| Speed of sound (c_∞) | 343 m/s |

For uniform inflow distribution we consider a condition in which the free-stream velocity vector, \mathbf{V}_∞ , is parallel to the blade rotational axis. On the other hand, a non-uniform inflow distribution consists of a free stream velocity vector which has an inclination, α , with respect to the propeller axis.

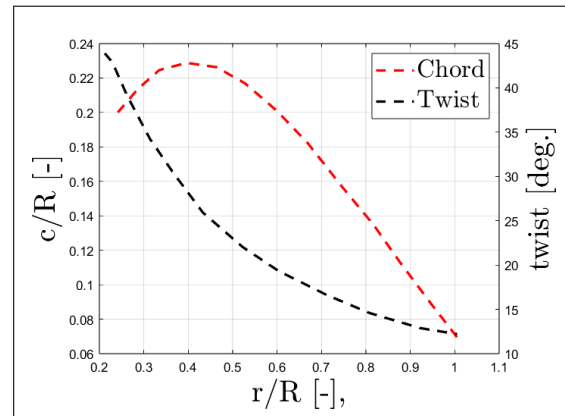


Figure 2. Blade geometry.

First, a comparison of the thrust coefficient C_T , the torque coefficient C_Q and the propulsive efficiency η , for different advance ratios J , calculated as in Eqn. (3), is shown in Fig. 3, Fig. 4 and Fig. 5. Here, the rotor is kept at a constant angular velocity of 4000 rpm, and the results are compared with respect to experimental data [20].

$$C_T = \frac{T}{\rho n^2 D^4} \quad C_Q = \frac{Q}{\rho n^2 D^5} \quad \eta = J \frac{C_T}{C_Q} \quad (3)$$

The numerical results match well with the experimental ones. The thrust coefficient is overpredicted for low



FORUM ACUSTICUM EURONOISE 2025

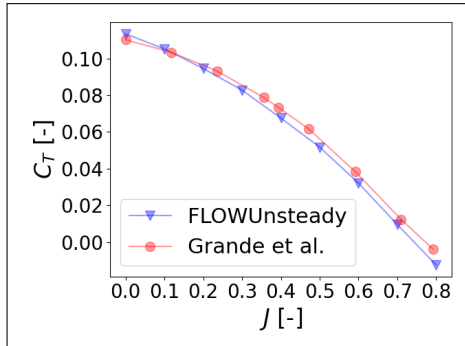


Figure 3. Thrust coefficient as a function of advance ratio.

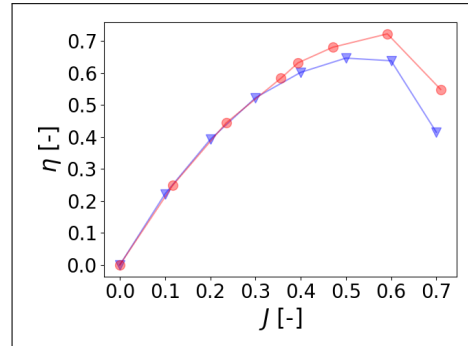


Figure 5. Propulsive efficiency as a function of advance ratio.

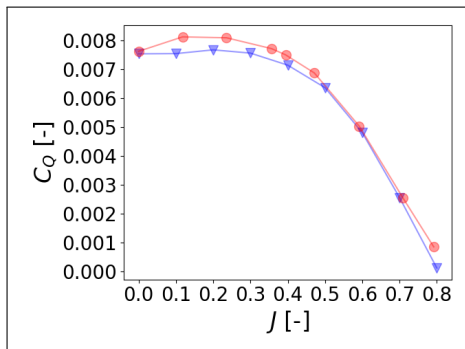


Figure 4. Torque coefficient as a function of advance ratio.

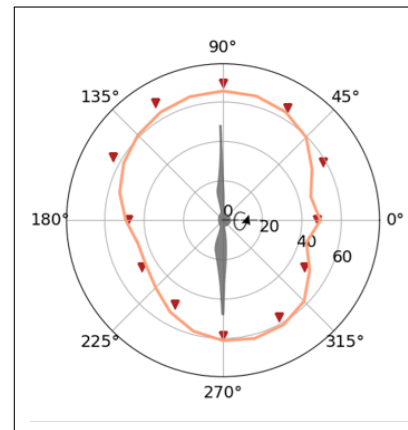


Figure 6. Thickness+Loading noise, $\alpha = 15^\circ$. Solid line represents low-fidelity results. Results are in dB.

advance ratios, while it is underpredicted for higher ones; while the torque coefficient is underpredicted for low advance ratios in the order of 7%. This behavior reflects in the propulsive efficiency.

Acoustic results are compared with high-fidelity ones from [4] in terms of SPL directivity, for a uniform inflow condition, $\alpha = 0^\circ$, and a non-uniform inflow condition, $\alpha = 15^\circ$, both at $J = 0.4$. Fig. 6 shows the SPL directivity for the non uniform inflow distribution, and we can see that the low-fidelity results, computed with the present framework, match quite well with the high-fidelity data from [4].

4. RESULTS

In this section, the effects of a short-time maneuver are investigated, i.e. an angular velocity variation, between two steady conditions at constant angular velocity, for the rotor geometry described above. The maneuver is shown

in Fig. 7.

Defined $t_{P_3} - t_{P_0}$ as the total time (t_{tot}) of the maneuver, and $t_{P_2} - t_{P_1}$ the transient time (Δt) between the two steady conditions, the transition between the two steady condition is obtained with different laws, a first order polynomial and a third order polynomial, and the transient time is varied in order to study the influence of both on physical noise metrics, such as SPL, and Sound Quality Metrics (SQM). In all the simulations the rotor position is fixed, with a uniform inflow ($V_x = V_\infty$) of 3 m/s, in order to speed up the convergence and eliminate the effects of a possible wake ingestion. The rotational speeds are set equal to $\Omega_{P_1} = 4000$ rpm $\Omega_{P_3} = 5000$ rpm. The selected transient times are $\Delta t = 0.1, 0.5$ s and the total time of the maneuver $t_{tot} = 1$ s. Tab. 2 summarizes the characteristic times, referring to Fig. 7, for each maneuver.





FORUM ACUSTICUM EURONOISE 2025

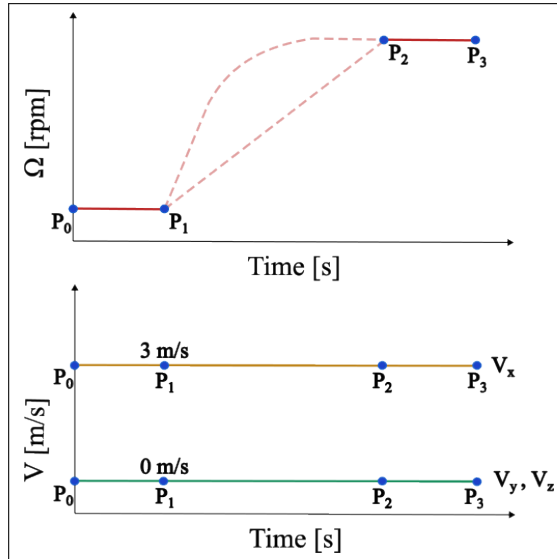


Figure 7. Reference maneuvers.

Table 2. Characteristic times of the maneuver.

| Δt (s) | t_{P_1} (s) | t_{P_2} (s) |
|----------------|---------------|---------------|
| 0.1 | 0.45 | 0.55 |
| 0.5 | 0.25 | 0.75 |

4.1 Physical Noise Metrics

In this section, the effect of the maneuver will be investigated in terms of SPL and its directivity. Fig. 8 and Fig. 9 show the directivity in time of the first order polynomial maneuver in terms of a difference in SPL, for the two transient times, defined as $\Delta SPL = SPL_{\Delta t=0.1} - SPL_{\Delta t=0.5}$, for the thickness and loading noise, respectively. Θ is the angle between the observer and the propeller axis, see Fig. 6 for reference. Observing the figures, it can be stated that in the two stationary conditions, the two maneuvers have the same SPL values, but because of the different transient time, these stationary conditions are reached at different times. In fact, observing Fig. 8, the ΔSPL decreases from 0.25s to 0.45s, approximately, becoming zero at 0.5s, and then starts to increase until 0.55s, where the maneuver with $\Delta t = 0.1s$ reaches the steady condition. This behavior appears to be independent of Θ , but dependent only on the angular speed value. Focusing on the loading noise, Fig. 9, we can observe an overshoot in SPL at the beginning and end of the tran-

sient of each maneuver. The overshoot seems to increase in magnitude and to affect a bigger range of Θ , decreasing the transient time. This behavior is related to the thrust derivative with respect to the retarded time in the FW-H equation, which becomes important approaching the propeller axis, and the effect becomes more evident as the transient time decreases.

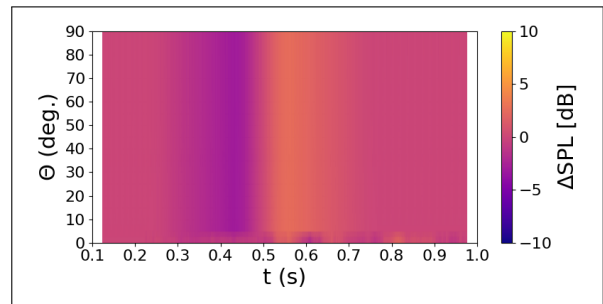


Figure 8. Thickness noise, first order polynomial.

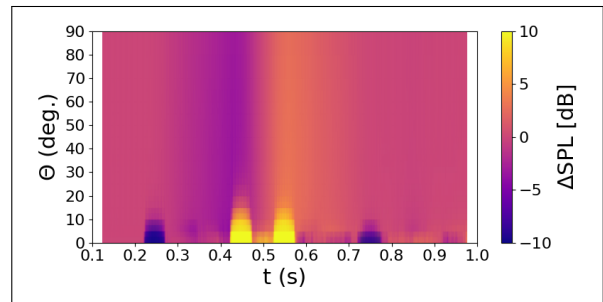


Figure 9. Loading noise, first order polynomial.

This effect can also be observed considering the spectrograms, Fig. 10 and Fig. 11, obtained for the first order polynomial transient with $\Delta t = 0.1s$. We can see that for $\Theta = 20^\circ$, Fig. 11, SPL is higher in two low-frequency bands at the beginning and end of the transient and disappear for $\Theta = 90^\circ$, Fig. 10.

The same behavior appears also for the third order polynomial at the beginning of the transient where the first order derivative of the thrust and angular velocity are greatest, Fig. 12.

Setting the transient time, it is possible to compare different transient laws, that are the third order polynomial and the first order polynomial, as presented in Fig. 7. Fig. 13 and Fig. 14 shows the thickness and loading noise, respectively, for $\Delta t = 0.5s$, in terms of $\Delta SPL =$



FORUM ACUSTICUM EURONOISE 2025

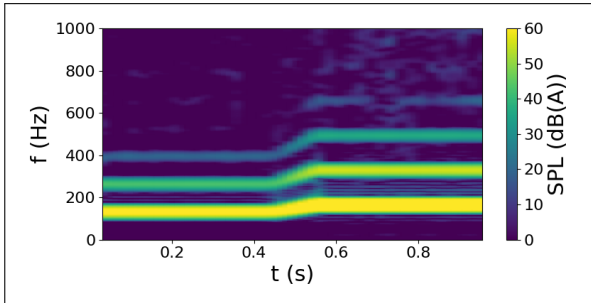


Figure 10. Spectrogram, poly1, $\Theta = 90^\circ$, $\Delta t = 0.1s$.

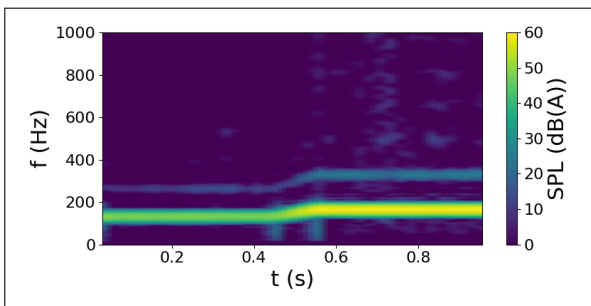


Figure 11. Spectrogram, poly1, $\Theta = 20^\circ$, $\Delta t = 0.1s$.

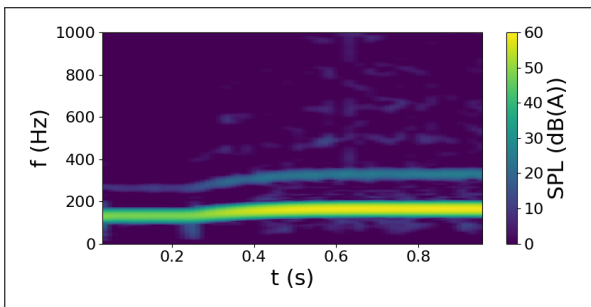


Figure 12. Spectrogram, poly3, $\Theta = 20^\circ$, $\Delta t = 0.5s$.

$SPL_{poly3} - SPL_{poly1}$, which is the difference between the third order polynomial SPL and the first order polynomial SPL. As can be seen, from $t = 0.25s$ to $t = 0.75s$ the ΔSPL is positive, while it is zero during the two steady conditions. That is because the transient of the third order polynomial is characterized by higher angular velocities. The same behavior can be observed for the loading noise, with some differences from $\Theta = 0^\circ$ to $\Theta = 90^\circ$. In fact,

for $t = 0.25s$ the SPL of the third order polynomial is higher with respect to the first order polynomial; while the opposite behavior is observed for $t = 0.75s$. These results reflect the effect of the thrust derivative, which is higher, for the third order polynomial, at the beginning of the transient, and it is zero at the end of the transient.

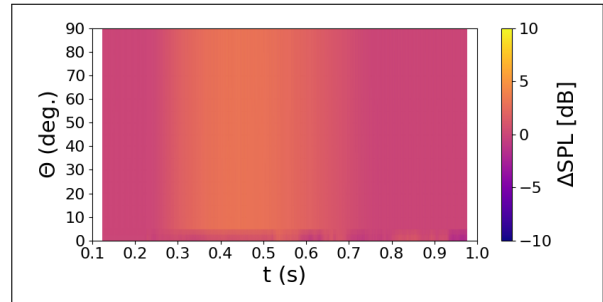


Figure 13. Thickness noise, $\Delta t = 0.5s$.

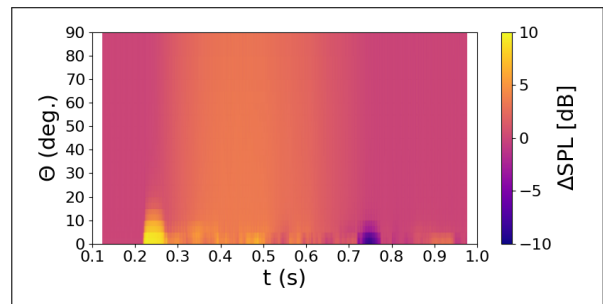


Figure 14. Loading noise, $\Delta t = 0.5s$.

4.2 Sound Quality Metrics

To understand if the effects described above affects the human perception, the SQM are analyzed. Fig. 15 and Fig. 16 show the loudness (ISO 532-1:2017) at $\Theta = 90^\circ$ and $\Theta = 20^\circ$, respectively. As can be seen, the loudness increases as the observer approaches the rotor disk and it is dependent on the angular velocity variation law. In fact, the third order polynomial transient is characterized by higher loudness with respect to the first order polynomial, reflecting the angular velocity transient law, while during the two steady conditions the loudness remains constant, as expected.

Looking at the sharpness (DIN.45692:2009), Fig. 17 and Fig. 18, a peak in the transient region of the maneuver is observed. Moreover, the shape of the curve and the



FORUM ACUSTICUM EURONOISE 2025

magnitude of the peak seems to be dependent on the time variation of the angular velocity of the rotor. In fact, fixing the transient time, the third order polynomial transient law is characterized by a higher peak and this can be related to the effect of the higher derivative of the angular velocity at the beginning of the transient. The same observation can be made fixing the transient law and reducing the transient time.

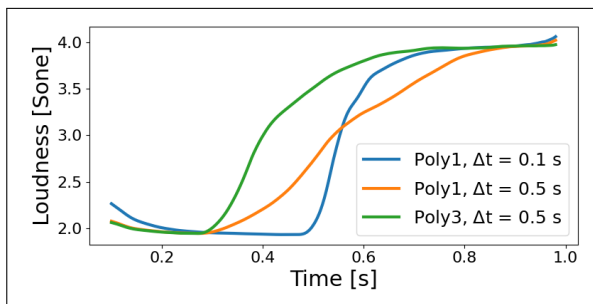


Figure 15. Loudness, $\Theta = 90^\circ$.

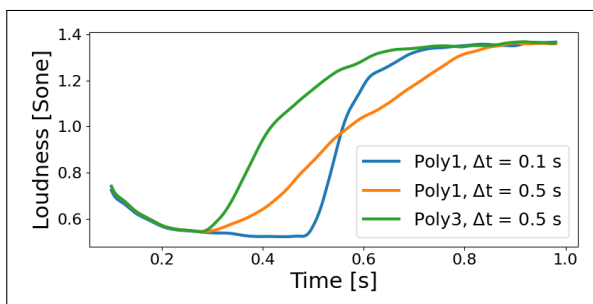


Figure 16. Loudness, $\Theta = 20^\circ$.

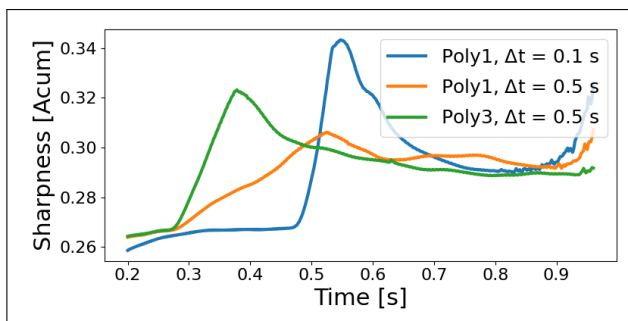


Figure 17. Sharpness, $\Theta = 90^\circ$.

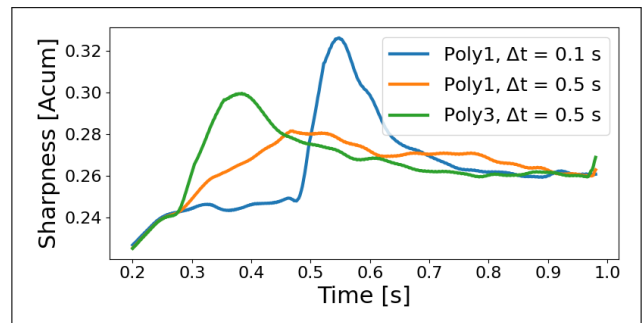


Figure 18. Sharpness, $\Theta = 20^\circ$.

5. CONCLUSIONS

In this paper we presented a mid/low-fidelity tool for noise prediction of eVTOL vehicles. The framework is based on a Vortex Particle Method and a time-domain Ffowks Williams and Hawkings analogy. The framework is validated with high-fidelity and experimental data for a single propeller in uniform and non-uniform inflow conditions. The good agreement of low-fidelity data with respect to the high-fidelity ones gave confidence in employing the tool for the study of a maneuver. The maneuver consists of an angular velocity transient between two steady conditions, and the objective was to understand if the transient time and the angular velocity law affects physical and Sound Quality metrics, for a single two-bladed propeller. In particular, we observed the following features:

- time-dependent SPL directivity: from $\Theta = 0^\circ$ to approx. $\Theta = 30^\circ$, we observed two overshoots in SPL at the beginning and end of the transient. These overshoots are characterized by low-frequency noise, caused by the time variation of the thrust of the rotor, which becomes important as the observer approaches the propeller axis;
- transient time dependence: reducing the transient time, the overshoots increase in magnitude, both for the SPL and the sharpness;
- transient law dependence: how the two steady conditions are reached seems to influence the SPL and the sharpness. Highest time derivative of the angular velocity causes higher overshoots in SPL and sharpness;
- the loudness shape seems to be dependent only by the angular velocity.



FORUM ACUSTICUM EURONOISE 2025

In order to understand if these effects affect the noise perception, more in depth studies should be conducted, like sound perception tests on a sample of individuals and more specific maneuvers, representative of real eVTOL flight scenarios.

6. ACKNOWLEDGEMENTS

This publication is part of the project PNRR-NGEU which has received funding from the MUR-DM 117/2023 and is co-funded by C.I.R.A.



7. REFERENCES

- [1] Y. Zhou, H. Zhao, and Y. Liu, "An evaluative review of the vtol technologies for unmanned and manned aerial vehicles," *Computer Communications*, vol. 149, 2019.
- [2] S. Hasan, "Urban air mobility (uam) market study," 2018. NASA Urban Air Mobility Report.
- [3] M. Al-Labbad, A. Wall, G. L. Larose, F. Khouli, and H. Barber, "Experimental investigations into the effect of urban airflow characteristics on urban air mobility applications," *Journal of Wind Engineering Industrial Aerodynamics*, vol. 229, 2022.
- [4] G. Romani, E. Grande, F. Avallone, D. Ragni, and D. Casalino, "Computational study of flow incidence effects on the aeroacoustics of low blade-tip mach number propellers," *Aerospace Science and Technology*, vol. 120, 2022.
- [5] P. W. Song, H. Z. Han, and D. Z. Qiao, "Prediction of hovering rotor noise based on reynolds-averaged navier-stokes simulation," *Journal Of Aircraft*, vol. 44, 2007.
- [6] J. Yangzhou, J. Wu, Z. Ma, and X. Huang, "Aeroacoustic sources analysis of wake-ingesting propeller noise," *Journal of Fluid Mechanics*, vol. 962, 2023.
- [7] M. J. Lighthill, "On sound generated aerodynamically i. general theory," in *Proc. of the Royal Society of London Series A, Mathematical and Physical Sciences*, 1952.
- [8] J. B. H. M. Schulten, "Frequency-domain method for the computation of propeller acoustics," *AIAA Journal*, vol. 26, 1988.
- [9] G. P. Succi, D. H. Munro, and J. A. Zimmer, "Experimental verification of propeller noise," *AIAA Journal*, vol. 20, 1982.
- [10] D. Boots and D. Feszty, "Numerical investigation of the effect of wing position on the aeroacoustic field of a propeller," in *Proc. of AIAA/SAE/ASSEE Joint Propulsion Conference*, (Salt Lake City, USA), 2016.
- [11] G. A. Bres, S. K. Brentner, G. Perez, and H. E. Jones, "Maneuvering rotorcraft noise prediction," *Journal of Sound and Vibration*, vol. 275, 2004.
- [12] H. Chen, S. K. Brentner, V. L. Lopes, and F. J. Horn, "An initial analysis of transient noise in rotorcraft maneuvering flight," *International Journal of Aeroacoustics*, vol. 5, 2006.
- [13] S. K. Brentner and F. Farassat, "Modeling aerodynamically generated sound of helicopter rotors," *Progress in Aerospace Sciences*, vol. 39, 2003.
- [14] O. Bergmann, F. Mohren, C. Braun, and F. Janser, "Propeller noise prediction for transient evtol mission," in *Proc. of AIAA SciTech Forum*, (Orlando, USA), 2024.
- [15] E. Gallo, G. Beaulieu, and C. Schram, "Annoyance factors of a maneuvering multicopter drone," in *Proc. of AIAA/CEAS Aeroacoustics Conference*, (Southampton, UK), 2022.
- [16] M. Snellen, R. Merino-Martinez, A. Altena, A. Amiri-Simkooei, C. Cappagli, A. Morin, L. Quaroni, F. Yunus, and R. Yupa-Villanueva, "Research on drone and urban air mobility noise: Measurement, modelling, and human perception," in *Proc. of Quietdrones Conference*, (Manchester, UK), 2024.
- [17] E. J. Alvarez, *Reformulated Vortex Particle Method and Meshless Large Eddy Simulation of Multirotor Aircraft*. Ph.D. dissertation, Brigham Young University, Provo, UT, 2022.
- [18] S. Glegg and W. Devenport, *Aeroacoustics of Low Mach Number Flows*. Academic Press, 2017.
- [19] Green Forge Coop., "Mosquito."





FORUM ACUSTICUM EURONOISE 2025

- [20] E. Grande, G. Romani, D. Ragni, F. Avallone, and D. Casalino, "Aeroacoustic investigation of a propeller operating at low Reynolds numbers," *AIAA Journal*, vol. 60, 2022.



11th Convention of the European Acoustics Association
Málaga, Spain • 23rd – 26th June 2025 •

